Kinetic Study of the Competitive Hydrogenation of Glycolaldehyde and Glucose on Ru/C with or Without AMT

Junying Zhang, Baolin Hou, Aiqin Wang, Zhenlei Li, Hua Wang, and Tao Zhang
State Key Laboratory of Catalysis, Dalian Institute of Chemical Physics, Chinese Academy of Sciences, Dalian 116023, China

DOI 10.1002/aic.14639
Published online October 10, 2014 in Wiley Online Library (wileyonlinelibrary.com)

The competitive hydrogenation of glycolaldehyde and glucose over 1% Ru/C catalyst was studied in a batch reactor at 373–403 K and 6 MPa hydrogen pressure, with or without the presence of ammonium metatungstate (AMT). It was found that the presence of AMT retarded significantly the hydrogenation of both aldoses, and this suppressing effect was more pronounced on the glucose hydrogenation. The hydrogenation of glycolaldehyde occurred always preferentially to the glucose hydrogenation, with or without the presence of AMT. The kinetic data in the absence of AMT were well modeled based on Langmuir–Hinshelwood–Hougen–Watson kinetics assuming the surface reaction being rate-determining and noncompetitive adsorption of dissociatively chemisorbed hydrogen and aldose. However, in the presence of AMT, the complexing between AMT and aldose and the strong adsorption of AMT on Ru surface must be considered in the development of new kinetic model. The as-modified model described the data satisfactorily. © 2014 American Institute of Chemical Engineers *AIChE J*, 61: 224–238, 2015
Keywords: glucose, glycolaldehyde, hydrogenation, kinetics, ethylene glycol

Introduction

Lignocellulose is being considered as a sustainable alternative to fossil feedstock for the production of fuels and chemicals. Various chem- and bio-transformation routes have been developed to this end,[1–31] among which the one-pot chemical transformation of cellulose to ethylene glycol (EG) and propylene glycol may provide a new route for the production of commodity chemicals from renewable biomass.[32–37] Although a great deal of efforts have been devoted to the design and development of effective and robust catalysts,[38–45] the reaction kinetics as well as the underlying mechanism implications have rarely been studied, possibly due to the complicated nature of the involved reactions.

For the one-pot conversion of cellulose to EG, there are three consecutive reactions: (1) hydrolysis of cellulose to glucose; (2) retro-aldol condensation of glucose to glycolaldehyde; and (3) hydrogenation of glycolaldehyde to EG.[35] In addition, several parallel side reactions are also involved to compete with the three main reactions, such as hydrogenation of glucose to sorbitol, and isomerization of glucose to fructose followed by subsequent hydrogenation to mannitol and sorbitol, as illustrated in Scheme 1.[46] The three main reactions are catalyzed by different active sites: the hydrolysis of cellulose is usually catalyzed by protons that are either *in situ* generated by hot water or provided by additional acid catalysts[4,5,14]; the retro-aldol condensation of glucose is effectively and uniquely catalyzed by tungstic compounds[35,42,45]; and the hydrogenation of glycolaldehyde is catalyzed by supported metal catalysts such as Ni and Ru. As such, the one-pot reaction from cellulose or glucose to EG necessitates the employment of bifunctional or dual catalysts. In our previous work, the dual catalysts composed of tungstic acid (H_2WO_4) and Ru/C or Raney Ni showed high activity, selectivity, and durability for the one-pot conversion of cellulose to EG.[42,45] Nevertheless, due to the temperature-controlled phase transfer behavior of tungstic acid, that is, it is insoluble in water at room temperature but becomes partially soluble during the reaction by transforming into tungsten bronze (H_xWO_3), it is quite difficult to precisely quantify the real catalyst amount. Therefore, in the kinetic studies of glucose conversion to EG, it is preferable to use a soluble tungstic compound as the catalyst component for retro-aldol condensation of glucose. Furthermore, the reaction tests with various tungstic compounds (WC_x, WO_3, H_2WO_4, $H_4O_{40}PW_{12}$, $(NH_4)_6H_2W_{12}O_{40}$, etc.) showed that the EG yields were comparable.[45] Based on these considerations, in the first part of the kinetic studies,[46] we used ammonium metatungstate (AMT) (abbreviated as AMT, the chemical formula $(NH_4)_6H_2W_{12}O_{40}$) as the sole catalyst component to study the kinetics of glucose retro-aldol condensation. The results showed that the activation energy for glucose retro-aldol condensation was as high as 141.3 kJ/mol and the reaction was first-order with respect to glucose and only moderately dependent on the AMT concentration (0.257th-order). These kinetic parameters strongly indicate that the occurrence of retro-aldol condensation of glucose requires a high temperature, and our experiments proved that the optimum temperature for EG production from cellulose was between 513 and 533 K.[32]

Correspondence concerning this article should be addressed to T. Zhang at taozhang@dicp.ac.cn and A. Wang at aqwang@dicp.ac.cn.

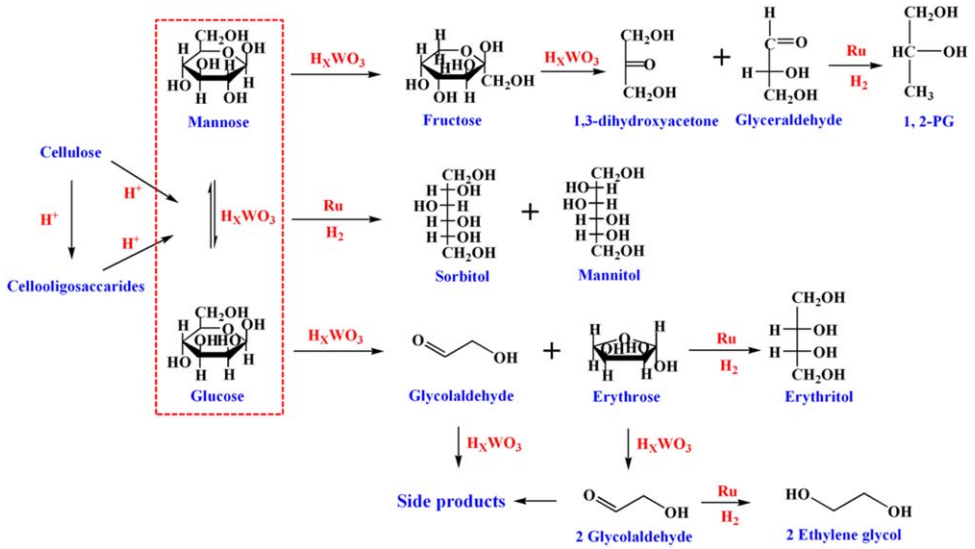

Scheme 1. The reaction network of cellulose transformation with dual catalyst $HxWO_3$ + Ru.[46]

[Color figure can be viewed in the online issue, which is available at wileyonlinelibrary.com.]

To obtain the detailed kinetics of the overall reaction from glucose to EG, following the kinetics of retro-aldol condensation of glucose in previous work,[46] we studied the kinetics of the competitive hydrogenation of glycolaldehyde and glucose under the presence of dual catalyst AMT + Ru/C, and the results are reported herein. In the one-pot conversion of glucose to EG, one of the main side reactions is the hydrogenation of glucose to sorbitol, which competes with the hydrogenation of glycolaldehyde over the same Ru surface.[35] Therefore, how to suppress the hydrogenation of glucose is the key to enhancing the selectivity to EG, as shown in reaction Scheme 2. The kinetic study of the competitive hydrogenation of glucose and glycolaldehyde is expected to provide useful information to this end.

At first sight, the kinetics of sugar hydrogenation is simple and well-defined kinetic models have been developed,[47–55] for example, for the hydrogenation of glucose over Ni or Ru catalysts.[47–52] However, in this work, we have for the first time found that the presence of AMT, which is one constituent of the dual catalyst for the one-pot conversion of cellulose/glucose to EG, retarded significantly the hydrogenation of sugars, especially for the hydrogenation of glucose. In this case, traditional kinetic models cannot be directly applied to the hydrogenation of sugars. New kinetic models must be developed.

Crezee et al. made a detailed study on the mass transfer and kinetics of three-phase hydrogenation of D-glucose over a 5% Ru/C catalyst at 373–403 K, 4.0–7.5 MPa H_2 pressure, and D-glucose concentration of 0.56–1.39 mol/L.[52] According to their results, the hydrogenation reaction rate was first-order with respect to hydrogen, but it showed a shift in the reaction order with respect to glucose from first-order at low concentrations (<0.3 mol/L) to zero order at high concentrations. The observed activation energy was 55 kJ/mol which was much bigger than the activation energy of diffusion in liquids (12–21 kJ/mol[51]), confirming the chemical kinetics control. Three different models based on Langmuir–Hinshelwood–Hougen–Watson (LHHW) kinetics, including noncompetitive adsorption of hydrogen and glucose (Model 1), competitive adsorption of molecular hydrogen and glucose (Model 2), and competitive adsorption of dissociatively chemisorbed hydrogen and glucose (Model 3), were used to describe the kinetics of D-glucose hydrogenation, and they were all found to model the data satisfactorily.[52] Also using a 5% Ru/C as the catalyst, Kuusisto et al. studied the kinetics of D-lactose hydrogenation at 383–403 K and 40–60 bar hydrogen.[55] The kinetic data were well modeled by LHHW kinetics assuming noncompetitive adsorption of molecular hydrogen and lactose on the catalyst surface. The apparent activation energy was in the range of 54–73 kJ/mol, and the reaction rate was first-order with respect to both hydrogen and lactose. Chang et al. studied the kinetics of the hydrogenation of four different ketones over Raney Ni catalyst via the initial-rate method.[56] The four hydrogenation reactions were successfully described by L-H kinetic model assuming the surface reaction of adsorbed ketone molecules and adsorbed hydrogen atoms being the rate-determining step. They further successfully applied this model to describe the kinetics of the mixture of four ketones.

Different from the extensive kinetic study of glucose hydrogenation, the hydrogenation of glycolaldehyde has rarely been reported. Glycolaldehyde is the simplest aldose molecule containing two carbon atoms. Compared with other sugars, it is more reactive toward oxidation, condensation, hydrogenation, and other chemical transformations. For example, it was reported that lactic acid can be formed in a yield of 28%

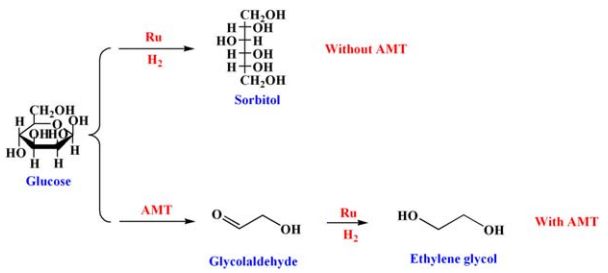

Scheme 2. Competitive hydrogenation of glucose and glycolaldehyde over Ru/C catalyst with or without the presence of AMT.

[Color figure can be viewed in the online issue, which is available at wileyonlinelibrary.com.]

from glycolaldehyde through aldol condensation in alkaline hydrothermal conditions.[57] Delidovich et al. further investigated the kinetics for the condensation of glycolaldehyde with formaldehyde in a weakly alkaline medium and found that the reaction order with respect to glycolaldehyde was unity.[58] On the other hand, inspired by formose-based hypotheses surrounding the origin of life,[59] Dusselier et al. developed a new catalytic route starting from glycolaldehyde toward a series of α-hydroxy acids and their esters using Sn-based catalysts.[60] In the context of the bio-oil upgrading, glycolaldehyde was also used as a model compound in the bio-oil for study its hydrogenation performance, and a high yield of EG was obtained at a reaction temperature of 363–418 K and a H_2 pressure of 10 bar using a homogeneous Ru catalyst.[61] Nevertheless, no kinetic data were reported.

In this work, the kinetics of hydrogenation reactions of glycolaldehyde and glucose as well as their mixture over a 1% Ru/C catalyst are studied with or without the presence of AMT. This study, together with the kinetic result of retro-aldol condensation of glucose described in previous work,[46] will provide a clear image for the mechanism understanding and kinetic correlations of the one-pot conversion of cellulose and glucose to EG, and therefore, can pave the way for the industrial application of sustainable production of EG from biomass.

Methods

Reaction tests

As described in our previous work,[46] the hydrogenation reactions of glucose (J & K Chemical) and glycolaldehyde (Chemfun Medical Technology Co., Shanghai) were conducted in a batch reactor of stainless-steel autoclave (Parr Instrument Company, 300 mL) which is equipped with sampling tube, stirring impeller, and temperature and pressure control system. For each reaction, 0.20 g 1% Ru/C (Shanxi Rock New Materials Co.), 0.05 g AMT (added only when considering the effect of AMT), and 140 mL water were put into the autoclave. The autoclave was flushed with H_2 five times and then sealed. After the autoclave was heated to the desired temperature, pure H_2 gas was charged until the pressure of 6 MPa. Ten milliliters of an aqueous solution of glucose or glycolaldehyde or a mixture of glucose and glycolaldehyde was fed into the autoclave by a Shimadzu LC pump (LC-20A) at a flow rate of 10 mL/min. It took 1 min to finish the feeding process, and this point was considered as the initial time ($t = 0$). Then, the reaction was started by strong agitation at 1100 rpm. Samples were taken from the reactor at a certain time interval for analysis.

Products analysis

After filtration through a 0.45 μm PTFE filter, the liquid samples were analyzed with a high performance liquid chromatograph (HPLC, Aglient 1200), with water as the mobile phase and refractive index (RI) as the detector. For the separation of products, a Shodex SC100 column was used with water flow rate of 0.6 mL/min and column temperature of 348 K. The quantification of products was made by an external standard method.

Kinetics model development

Aldoses Hydrogenation Without the *Presence of AMT*. Based on the previous reports on the kinetics of glucose hydrogenation[47–52] or ketones hydrogenation,[56] we used

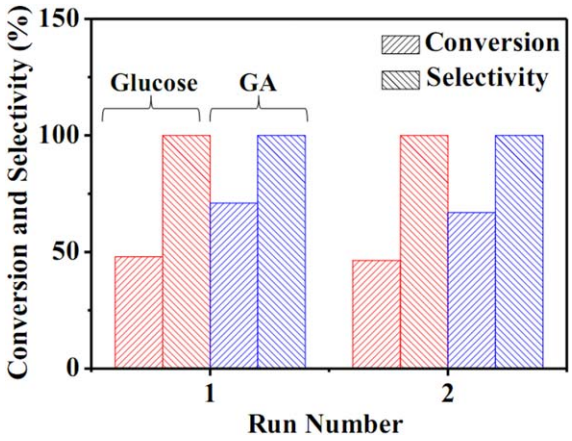

Figure 1. The recycling ability of Ru/C in glucose and glycolaldehyde hydrogenation.

Conditions: $T = 373$ K, $P_H = 6.0$ MPa, 2.0 g glucose (1.0 g glycolaldehyde), 0.2 g 1% Ru/C, 100 mL H_2O, 40 min. [Color figure can be viewed in the online issue, which is available at wileyonlinelibrary.com.]

LHHW model to describe the kinetics of aldoses (glucose and glycolaldehyde) hydrogenation considering the following assumptions: (i) the reaction is 100% selective to EG for glycolaldehyde hydrogenation and 100% selective to sorbitol for glucose hydrogenation; (ii) no catalyst deactivation occurs during the reaction; (iii) both glycolaldehyde and glucose are molecularly adsorbed while H_2 is dissociatively adsorbed on the Ru surface, and the adsorption between aldose and hydrogen is noncompetitive; (iv) the surface reaction between the adsorbed glycolaldehyde/glucose and hydrogen atom is the rate-determining step; and (v) there is negligible adsorption of solvent and product. The assumptions (i) and (ii) were justified by the hydrogenation tests in the batch reactor. For both glucose and glycolaldehyde hydrogenations, the selectivities to sorbitol and EG were all 100%, and no any byproduct was detected by HPLC. To evaluate the reaction stability, a higher aldose/Ru ratio was used to maintain the conversion of aldose below 100%. As shown in Figure 1, the Ru/C catalyst after the first run was submitted to the second run, and either the conversions of aldoses or the selectivities of sorbitol (or EG) remain essentially unchanged, demonstrating that the catalyst was rather stable and no any deactivation occurred during the reaction. As for the assumption (iii), considering that the dissociated hydrogen atom is far smaller than glycolaldehyde or glucose, the assumption of noncompetitive adsorption is reasonable and has also been adopted in many earlier reports.[50,52,55]

Based on the above model and assumptions, the reaction rates for individual glycolaldehyde and glucose hydrogenation can be expressed as

$$r_{GA} = k_{GA} \frac{K_H P_H}{(1+\sqrt{K_H P_H})^2} \frac{K_{GA} C_{GA}}{(1+K_{GA} C_{GA})} \quad (1)$$

$$r_G = k_G \frac{K_H P_H}{(1+\sqrt{K_H P_H})^2} \frac{K_G C_G}{(1+K_G C_G)} \quad (2)$$

where k_{GA} and k_G are the rate constants for glycolaldehyde hydrogenation and glucose hydrogenation, respectively; K_H, K_{GA}, and K_G are the adsorption equilibrium constants of hydrogen, glycolaldehyde, and glucose, respectively; and P_H,

C_{GA}, and C_G are the hydrogen partial pressure, glycolaldehyde concentration, and glucose concentration, respectively.

The partial pressure of H_2 is used in the above rate expressions in place of the hydrogen concentration in the liquid phase considering that Henry's law is effective in this case and Henry's law constant is incorporated in K_H. In addition, as the hydrogen concentration in the liquid phase was several orders of magnitude lower than the glycolaldehyde or glucose concentration,[52] the hydrogen adsorption term in the denominator was negligible compared to the glycolaldehyde or glucose adsorption term. Thus, the rate expressions can be further simplified as

$$r_{GA} = k_{GA}\frac{K_H P_H K_{GA} C_{GA}}{(1+K_{GA}C_{GA})} \tag{3}$$

$$r_G = k_G\frac{K_H P_H K_G C_G}{(1+K_G C_G)} \tag{4}$$

And the mass balances of glycolaldehyde and glucose take the following form

$$\frac{dC_{GA}}{dt} = -r_{GA}\,\rho_{cat} \tag{5}$$

$$\frac{dC_G}{dt} = -r_G\,\rho_{cat} \tag{6}$$

The temperature dependencies of k_{GA}, k_G, K_H, K_{GA}, and K_G in Eqs. 3 and 4 are described as follows

$$k_i = A_i e^{\frac{-E_{ai}}{RT}} \tag{7}$$

$$K_j = a_j e^{\frac{-\Delta H_j}{RT}} \tag{8}$$

where A_i (i = GA, G) is the pre-exponential factor; E_{ai} is the activation energy (kJ/mol); a_j (j = H, GA, G) is the pre-exponential factor in Van 't Hoff equation, ΔH_j is the adsorption enthalpy (kJ/mol). R is the ideal gas law constant (8.3143×10^{-3} kJ/mol K); T is the temperature (K).

Aldoses Hydrogenation with the Presence of AMT. In the presence of AMT, the complexing effect between AMT and aldose and the poisoning effect of AMT on the Ru/C surface are considered based on the previous study[46] as well as the control experiments below. Thereby, we make the following assumptions to develop the new kinetic model: (i) AMT is adsorbed on the surface of Ru/C; (ii) free or adsorbed AMT can bind glucose molecules step by step until a maximum of 4; (iii) the complex formed by coordination of AMT and glucose in solution can also be adsorbed on the Ru/C surface; (iv) the kinetics of the hydrogenation of AMT-coordinated glucose follows the LHHW model; and (v) the surface reaction is the rate-determining step.

With these assumptions, the elementary steps for glucose hydrogenation on the Ru/C catalyst under the presence of AMT can be described by the following equations

$$AMT + * \overset{K_{AMT}}{\rightleftharpoons} AMT* \tag{9}$$

$$AMT* + G \overset{K_1}{\rightleftharpoons} AMTG* \tag{10}$$

$$AMTG* + G \overset{K_2}{\rightleftharpoons} AMTG2* \tag{11}$$

$$AMTG2* + G \overset{K_3}{\rightleftharpoons} AMTG3* \tag{12}$$

$$AMTG3* + G \overset{K_4}{\rightleftharpoons} AMTG4* \tag{13}$$

$$AMT + 4G \overset{K_5}{\rightleftharpoons} AMTG4 \tag{14}$$

$$AMTG4 + * \overset{K_6}{\rightleftharpoons} AMTG4* \tag{15}$$

$$AMTG4* + 2H* \xrightarrow{k_7} AMTG3* + S* \tag{16}$$

$$AMTG3* + 2H* \xrightarrow{k_8} AMTG2* + S* \tag{17}$$

$$AMTG2* + 2H* \xrightarrow{k_9} AMTG* + S* \tag{18}$$

$$AMTG* + 2H* \xrightarrow{k_{10}} AMT* + S* \tag{19}$$

$$G + * \overset{K_G}{\rightleftharpoons} G* \tag{20}$$

$$H_2 + * \overset{K_H}{\rightleftharpoons} 2H* \tag{21}$$

$$G* + 2H* \xrightarrow{k_G} S* + * \tag{22}$$

$$S* \overset{K_S}{\rightleftharpoons} S + * \tag{23}$$

As the surface reaction is the rate-determining step, the adsorption equilibria for glucose, AMT-binded compounds, and hydrogen on Ru/C are achieved, and the rate expressions becomes:

$$K_{AMT}\ C_{AMT}\ \theta_{V1} = \theta_{AMT} \tag{24}$$

$$\theta_{AMTG} = K_1\theta_{AMT}C_G \tag{25}$$

$$\theta_{AMTG2} = K_1\ K_2\ \theta_{AMT}{C_G}^2 \tag{26}$$

$$\theta_{AMTG3} = K_1K_2K_3\ \theta_{AMT}{C_G}^3 \tag{27}$$

$$\theta_{AMTG4} = K_1K_2K_3K_4\ \theta_{AMT}{C_G}^4 \tag{28}$$

$$K_5 C_{AMT}{C_G}^4 = C_{AMTG4} \tag{29}$$

$$K_6\ C_{AMTG4}\ \theta_{V1} = \theta_{AMTG4} \tag{30}$$

$$K_G\ C_G\ \theta_{V1} = \theta_G \tag{31}$$

$$\theta_{AMTG4} = K_6K_5C_{AMT}{C_G}^4\ \ \theta_{V1} \tag{32}$$

$$\theta_{AMTG3} = \frac{K_6K_5C_{AMT}{C_G}^4\ \theta_{V1}}{K_4C_G} \tag{33}$$

$$\theta_{AMTG2} = \frac{K_6K_5C_{AMT}{C_G}^4\ \theta_{V1}}{K_4K_3{C_G}^2} \tag{34}$$

$$\theta_{AMTG} = \frac{K_6K_5C_{AMT}{C_G}^4\ \theta_{V1}}{K_4K_3K_2{C_G}^3} \tag{35}$$

$$K_{AMT}C_{AMT}\theta_{V1} = \theta_{AMT} \tag{36}$$

$$K_H P_H \theta_{V2} = \theta_H \tag{37}$$

The balance of the catalyst sites is necessary to relate all the species adsorbed on the surface

$$\theta_{AMT}+\theta_{AMTG}+\theta_{AMTG2}+\theta_{AMTG3}+\theta_{AMTG4}+\theta_G+\theta_S+\theta_{V1}=1 \tag{38}$$

The noncompetitive adsorption between hydrogen and glucose leads to

$$\theta_{V2}+\theta_H=1 \tag{39}$$

As the adsorption of sugar alcohols (sorbitol) is much weaker than that of sugars (glucose), the balance of the catalyst sites becomes

$$\theta_{AMT}+\theta_{AMTG}+\theta_{AMTG2}+\theta_{AMTG3}+\theta_{AMTG4}+\theta_G+\theta_{V1}=1 \tag{40}$$

Considering that the AMT and Ru/C had been mixed adequately prior to the glucose being fed into the reactor, most of the AMT was strongly adsorbed on the Ru/C surface, which would decrease greatly the probability of the interaction between free AMT and glucose. Thus

$$K_6K_5 \ll K_4K_3K_2, K_4K_3, K_4 \tag{41}$$

Then, the equations become

$$\theta_{AMTG3}=\frac{K_6K_5C_{AMT}{C_G}^4\ \theta_{V1}}{K_4C_G} \approx 0 \tag{42}$$

$$\theta_{AMTG2}=\frac{K_6K_5C_{AMT}{C_G}^4\ \theta_{V1}}{K_4K_3{C_G}^2} \approx 0 \tag{43}$$

$$\theta_{AMTG}=\frac{K_6K_5C_{AMT}{C_G}^4\ \theta_{V1}}{K_4K_3K_2{C_G}^3} \approx 0 \tag{44}$$

Finally, the balance of the catalyst sites becomes

$$\theta_{AMT}+\theta_{AMTG4}+\theta_G+\theta_{V1}=1 \tag{45}$$

Therefore,

$$\theta_{V1}=\frac{1}{1+K_6K_5C_{AMT}{C_G}^4+K_GC_G+K_{AMT}C_{AMT}} \tag{46}$$

And the rate expression for glucose hydrogenation becomes

$$\begin{aligned} r_{G-AMT}&=r_{AMTG}+r_{AMTG2}+r_{AMTG3}+r_{AMTG4}+r_{G0}\\ &=k_{10}\theta_H\theta_{AMTG}+k_9\theta_H\theta_{AMTG2}+k_8\theta_H\theta_{AMTG3}\\ &\quad+k_7\theta_H\theta_{AMTG4}+k_G\theta_H\theta_G=k_7\theta_H\theta_{AMTG4}+k_G\theta_H\theta_G \end{aligned} \tag{47}$$

We assume that the binding of AMT with glucose does not affect the surface reaction rate constant between adsorbed glucose and hydrogen, that is, $k_7=k_8=k_9=k_{10}=k_G$, then the rate expression becomes

$$r_{G-AMT}=k_G\theta_H(\theta_{AMTG4}+\theta_G) \tag{48}$$

For convenience, we define the adsorption equilibrium constant: $K_5K_6=K_{G-AMT}$. Hence, the reaction rate for glucose hydrogenation can be described as

$$r_{G-AMT}=k_G\ \frac{K_HP_H}{(1+\sqrt{K_HP_H})^2}\frac{(K_{G-AMT}C_{AMT}{C_G}^4+K_GC_G)}{(1+K_{G-AMT}C_{AMT}{C_G}^4+K_GC_G+K_{AMT}C_{AMT})} \tag{49}$$

The hydrogen adsorption term in the denominator was negligible compared to the glucose adsorption term, and then the equation can be further simplified as

$$r_{G-AMT}=k_G\frac{K_HP_H(K_{G-AMT}C_{AMT}{C_G}^4+K_GC_G)}{1+K_{G-AMT}C_{AMT}{C_G}^4+K_GC_G+K_{AMT}C_{AMT}} \tag{50}$$

Similar to kinetic model development for glucose hydrogenation, we make the following assumptions for development of kinetic model of glycolaldehyde hydrogenation in the presence of AMT: (i) AMT is adsorbed on the surface of Ru/C; (ii) free or adsorbed AMT can coordinate glycolaldehyde with a stoichiometric ratio of 1/1; (iii) the complex formed by coordination of AMT and glycolaldehyde in solution can also be adsorbed on the Ru/C surface; (iv) the kinetics of the hydrogenation of AMT-coordinated glycolaldehyde follows the LHHW model; and (v) the surface reaction is the rate-determining step. Based on these assumptions and LHHW kinetic model, the elementary steps for glycolaldehyde hydrogenation on the Ru/C catalyst under the presence of AMT can be described by the following equations

$$AMT+GA*\overset{K_{11}}{\rightleftharpoons}AMTGA \tag{51}$$

$$AMTGA+*\overset{K_{12}}{\rightleftharpoons}AMTGA* \tag{52}$$

$$AMT+*\overset{K_{AMT}}{\rightleftharpoons}AMT* \tag{53}$$

$$AMT*+GA\overset{K_{13}}{\rightleftharpoons}AMTGA* \tag{54}$$

$$AMTGA*+2H*\xrightarrow{k_{14}}AMT*+EG* \tag{55}$$

$$GA+*\overset{K_{GA}}{\rightleftharpoons}GA* \tag{56}$$

$$H_2+*\overset{K_H}{\rightleftharpoons}2H* \tag{57}$$

$$GA*+2H*\xrightarrow{k_{GA}}EG*+* \tag{58}$$

$$EG*\overset{K_{EG}}{\rightleftharpoons}EG+* \tag{59}$$

As the surface reaction is the rate-determining step, the adsorption equilibria are achieved. As such, the rate expressions become

$$C_{AMTGA}=K_{11}\ C_{AMT}\ C_{GA} \tag{60}$$

$$\theta_{AMTGA}=K_{12}\ C_{AMTGA}\ \theta_{V1} \tag{61}$$

$$\theta_{AMT}=K_{AMT}\ C_{AMT}\ \theta_{V1} \tag{62}$$

$$\theta_{AMTGA}=K_{13}\ C_{GA}\ \theta_{AMT} \tag{63}$$

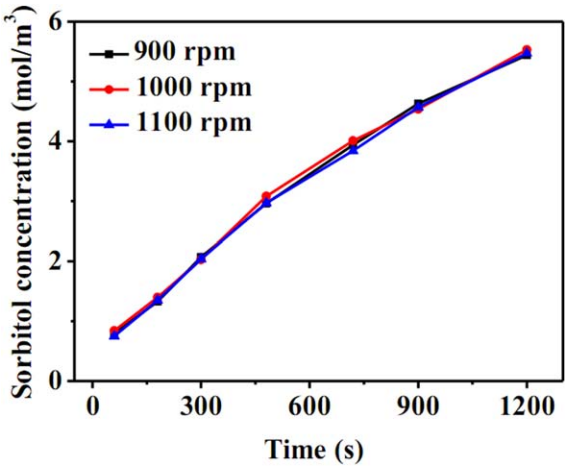

Figure 2. Effect of agitation speed on the product concentration of glucose hydrogenation.

Reaction conditions: $T = 403$ K, $P_H = 6.0$ MPa, $C_{G0} = 9.92$ mol/m^3, 0.2 g 1% Ru/C. [Color figure can be viewed in the online issue, which is available at wileyonlinelibrary.com.]

$$\theta_{GA} = K_{GA}\ C_{GA}\ \theta_{V1} \tag{64}$$

$$K_H P_H \theta_{V2} = \theta_H \tag{65}$$

The balance of the catalyst sites is necessary to relate all the species adsorbed on the surface

$$\theta_{AMTGA} + \theta_{AMT} + \theta_{GA} + \theta_{EG} + \theta_{V1} = 1 \tag{66}$$

Based on the noncompetitive adsorption between hydrogen and glycolaldehyde

$$\theta_{V2} + \theta_H = 1 \tag{67}$$

Considering that the adsorption of EG on Ru surface is much weaker than that of glycolaldehyde, the balance of the catalyst sites becomes

$$\theta_{AMTGA} + \theta_{AMT} + \theta_{GA} + \theta_{EG} + \theta_{V1} = 1 \tag{68}$$

Resolve the above equations, one can obtain

$$\theta_{V1} = \frac{1}{1 + K_{11}K_{12}C_{AMT}C_{GA} + K_{GA}C_{GA} + K_{AMT}C_{AMT}} \tag{69}$$

We assume that the binding of AMT with glycolaldehyde does not affect the surface reaction rate constant between adsorbed glycolaldehyde and hydrogen, that is, $k_{14} = k_{GA}$. Moreover, for convenience we define $K_{11}K_{12} = K_{GA-AMT}$. Then, the rate expression for glycolaldehyde hydrogenation becomes

$$\begin{aligned} r_{GA-AMT} &= r_{AMTGA} + r_{GA} = k_{14}\theta_H\theta_{AMTGA} + k_{GA}\theta_H\theta_{GA} = k_{GA}\theta_H\ (\theta_{AMTGA} + \theta_{GA}) \\ &= k_{GA}\frac{K_H P_H}{(1+\sqrt{K_H P_H})^2}\ \frac{K_{GA-AMT}C_{AMT}C_{GA} + K_{GA}C_{GA}}{1 + K_{GA-AMT}C_{AMT}C_{GA} + K_{GA}C_{GA} + K_{AMT}C_{AMT}} \end{aligned} \tag{70}$$

The hydrogen adsorption term in the denominator is negligible compared to the glycolaldehyde adsorption term, then

$$r_{GA-AMT} = k_{GA}\frac{K_H P_H (K_{GA-AMT}C_{AMT}C_{GA} + K_{GA}C_{GA})}{1 + K_{GA-AMT}C_{AMT}C_{GA} + K_{GA}C_{GA} + K_{AMT}C_{AMT}} \tag{71}$$

The experimental data with and without AMT, respectively, were fitted with the above four kinetic models (Eqs. 3, 4, 50, and 71) using Microsoft Excel Solver pack as described by Kemmer and Keller.[62] Due to the constant value of hydrogen adsorption term in these equations, only two parameters are to be determined. During the fitting process, the sum of squared residuals is computed and minimized using the solver add-in to obtain the set of parameter values that best describes the experimental data. The initial parameter values were set as 0.1 for both parameters. The fitting procedure was repeated using different initial values, and the fitting result was found to be independent on the initial values, demonstrating the reliability of the fitting result.

Results and Discussion

Mass transfer effects

For the kinetic study, it is important to ensure that the rate data are obtained in the kinetically controlled regime. Therefore, prior to the kinetic study, the effects of mass transfer were investigated in the hydrogenation of glucose under the catalysis of Ru/C and AMT. Figures 2–4 show the effects of agitation speed, catalyst particle size, and catalyst loading on the reaction rates. It is clear that both external (gas–liquid and liquid–solid mass transfer) and internal diffusion limitations can be safely eliminated when the reaction was operated at a stirring speed above 900 rpm, catalyst loading in the range of 0.2–0.6 g, and catalyst particle size smaller than 74 μm (>200 mesh). Therefore, in the subsequent kinetic studies, all the hydrogenation reactions were performed at an

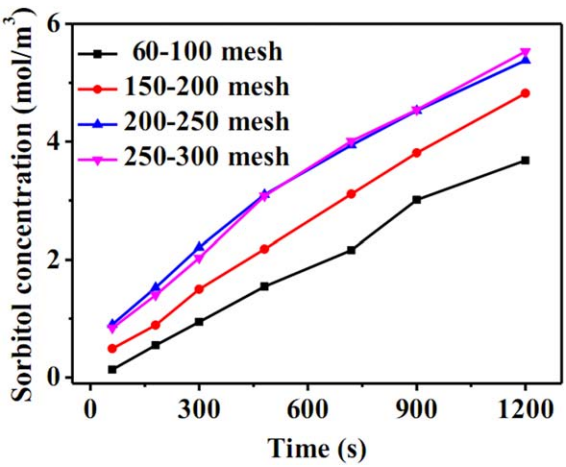

Figure 3. Effect of particle size on the product concentration of glucose hydrogenation.

Reaction conditions: $T = 403$ K, $P_H = 6.0$ MPa, $C_{G0} = 9.92$ mol/m^3, 0.2 g 1% Ru/C. [Color figure can be viewed in the online issue, which is available at wileyonlinelibrary.com.]

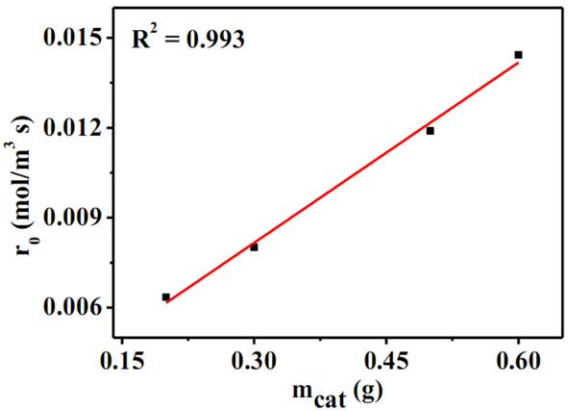

Figure 4. Effect of catalyst loading on the initial rate of glucose hydrogenation.

Reaction conditions: $T = 403$ K, $P_H = 6.0$ MPa, $C_{G0} = 9.92$ mol/m^3. [Color figure can be viewed in the online issue, which is available at wileyonlinelibrary.com.]

agitation speed of 1100 rpm, 1% Ru/C catalyst loading of 0.2 g, and the particle size of 250–300 mesh.

Kinetics of aldoses hydrogenation over Ru/C catalyst

Parameters Estimation. The kinetic experiments for individual hydrogenation of glycolaldehyde and glucose were conducted at 373–403 K and 6 MPa H_2 pressure, with 0.2 g 1% Ru/C as the catalyst. The initial concentrations of glycolaldehyde and glucose were 10.4 and 4.96 mol/m^3, respectively, and the H_2 pressure was kept at a constant value during the reaction. The kinetic models described in Eqs. 3 and 4 were used to fit the experimental data obtained at different temperatures. As the rate constants k_i (k_{GA} and k_G) and adsorption equilibrium constant of hydrogen (K_H) always appear as a product in the rate expressions and it is difficult to determine k_i and K_H separately, these parameters were lumped and expressed as k_iK_H. Thus, the parameters k_iK_H, K_{GA}, and K_G in the equations were determined by nonlinear least-squares fitting of the experimental data using Microsoft Excel Solver pack as described by Kemmer and Keller.[62] As shown in Figures 5 and 6, pretty good fitting results are obtained for both glycolaldehyde hydrogenation and glucose hydrogenation. As the concentration vs. time profiles look close to exponential, we also tried a simple one-parameter first-order irreversible model to fit the experimental data. Although the glucose hydrogenation can be described with the one-parameter model as well as that with two-parameter model, the glycolaldehyde hydrogenation cannot be fitted well with the one-parameter model probably because the glycolaldehyde adsorbs on Ru/C surface much stronger than glucose so that the $K_{GA}C_{GA}$ term in the denominator (Eq. 3) cannot be neglected. The parameters obtained with two-parameter models are summarized in Table 1. It can be seen that the adsorption equilibrium constant of glycolaldehyde (K_{GA}) is approximately twice as large as that of glucose (K_G), suggesting that the former molecules can be preferentially adsorbed on Ru surface than the latter. As a consequence, the rate constant of glycolaldehyde hydrogenation (k_{GA}) is also about twice as large as that of glucose hydrogenation (k_G). Thus, it can be anticipated that at comparable concentrations of glycolaldehyde and glucose the former hydrogenation rate is about four times faster than the latter. This result indicates that the glycolaldehyde is more competitive than glucose in the case of their mixture hydrogenation.

Crezee et al. reported a k_GK_H value of $(3.9 \pm 0.3) \times 10^{-4}$ mol/g$_{cat}$·bar·min when they used a similar model to evaluate the parameters in glucose hydrogenation over 5% Ru/C catalyst.[52] In our case, we obtained k_GK_H value of 2.28×10^{-6}

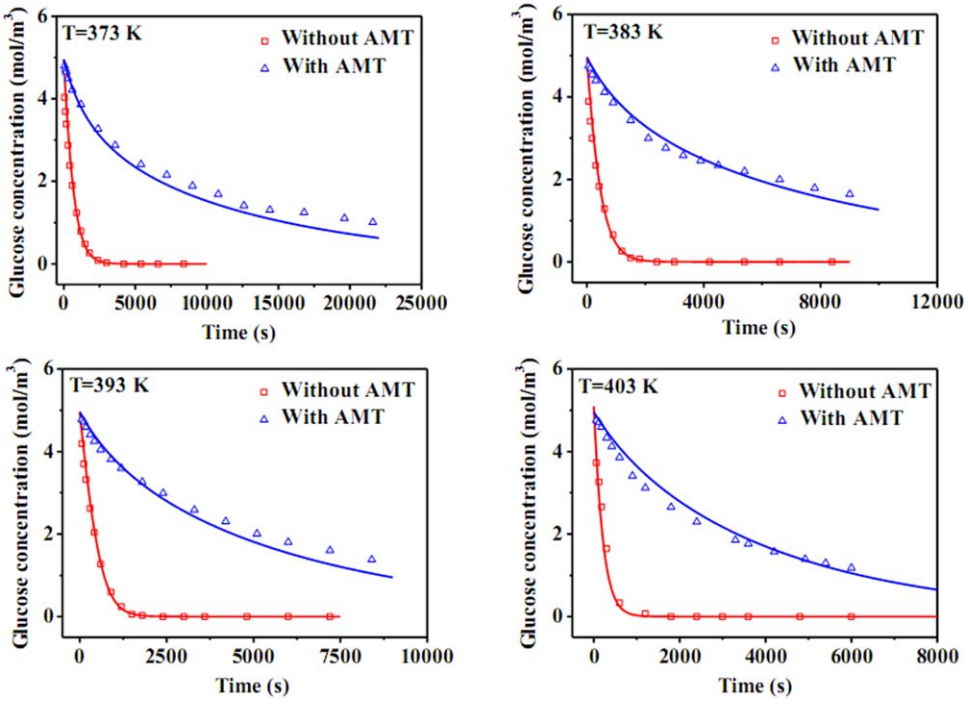

Figure 5. Experimental (dots) and fitting (lines) concentration profiles of glucose with and without AMT.

Reaction conditions: $C_{G0} = 4.96$ mol/m^3, $P_H = 6$ MPa, 0.2 g 1% Ru/C ($C_{AMT} = 0.11$ mol/m^3), 150 mL water, 1100 rpm. [Color figure can be viewed in the online issue, which is available at wileyonlinelibrary.com.]

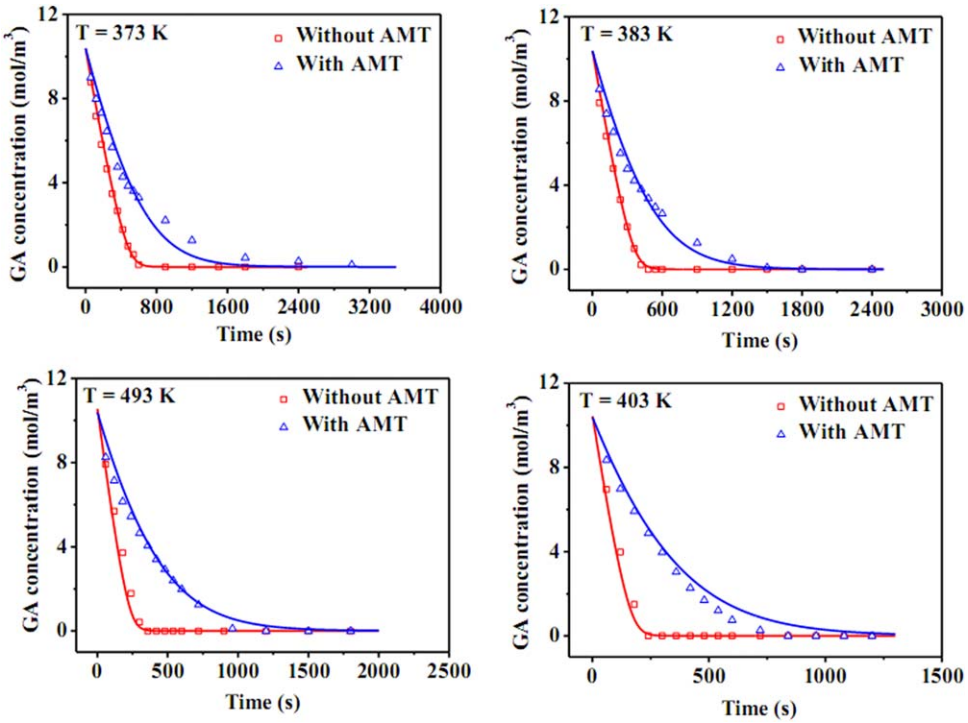

Figure 6. Experimental (dots) and fitting (lines) concentration profiles of glycolaldehyde with and without AMT.

Reaction conditions: $C_{GA0} = 10.4$ mol/m^3, $P_H = 6$ MPa, 0.2 g 1% Ru/C ($C_{AMT} = 0.11$ mol/m^3), 150 mL water, 1100 rpm. [Color figure can be viewed in the online issue, which is available at wileyonlinelibrary.com.]

mol/g_{cat}·bar·s over 1% Ru/C catalyst, which corresponds to 1.37×10^{-4} mol/g_{cat}·bar·min, slightly smaller than that reported by Crezee et al. However, taking into account the difference in the Ru loadings of the catalyst, our $k_G K_H$ value normalized by Ru loading will be twice as big as that obtained by Crezee et al. This is reasonable considering that the lower loading of Ru will lead to a higher dispersion and thereby a higher hydrogenation activity.

According to Arrhenius Eq. 7 and Van't Hoff Eq. 8, the parameters are estimated from the plots $\ln k_i K_H - 1/T$ and $\ln K_i - 1/T$, as shown in Figure 7. The apparent activation energies are 49.6 and 42.6 kJ/mol for glucose hydrogenation and glycolaldehyde hydrogenation, respectively. These values are very close to those in the literature.[47–52] Moreover, they are both much larger than the activation energy of diffusion in liquids (12–21 kJ/mol[51]), approving our data are obtained in the kinetic control region.

Model validation by the hydrogenation of glucose and glycolaldehyde mixture

For the one-pot conversion of cellulose to EG with the dual catalyst of AMT and Ru/C,[35] both the glucose and glycolaldehyde are produced as the intermediates which are subsequently transformed into sorbitol and EG, respectively, as shown in Schemes 1 and 2. Therefore, study of the competitive hydrogenation of glucose and glycolaldehyde over the Ru/C catalyst is very important to the understanding of the reaction mechanism as well as the design of a more selective catalyst. Herein, on the basis of the individual hydrogenation kinetics of glycolaldehyde and glucose, we perform the kinetic study of the mixture hydrogenation so as to validate the above-established model.

For the mixture of glucose and glycolaldehyde, the hydrogenation reaction rate can be expressed as

$$r_{G-m} = k_G \frac{K_H P_H K_G C_G}{(1 + K_G C_G + K_{GA} C_{GA})} \tag{72}$$

$$r_{GA-m} = k_{GA} \frac{K_H P_H K_{GA} C_{GA}}{(1 + K_G C_G + K_{GA} C_{GA})} \tag{73}$$

Compared with the individual hydrogenation rate expressions in Eqs. 3 and 4, one can clearly see that the competitive hydrogenation between glycolaldehyde and glucose suppresses the reaction rate, either for glycolaldehyde or glucose, as shown in Eqs. 74 and 75

$$\frac{r_{G-m}}{r_G} = \frac{1 + K_G C_G}{1 + K_G C_G + K_{GA} C_{GA}} < 1 \tag{74}$$

Table 1. Modeling Results for Individual Hydrogenation of Glucose and Glycolaldehyde Over Ru/C in the Absence of AMT

Model Equation	Parameter	Estimated Value			
		373 (K)	383 (K)	393 (K)	403 (K)
$r_G = k_G \frac{K_H P_H K_G C_G}{(1+K_G C_G)}$	$k_G K_H$ (mol/g_{cat} bar s)	1.01 E − 06	1.54 E − 06	2.28 E − 06	3.33 E − 06
	K_G (m^3/mol)	3.19 E − 01	2.78 E − 01	2.43 E − 01	2.15 E − 01
$r_{GA} = k_{GA} \frac{K_H P_H K_{GA} C_{GA}}{(1+K_{GA} C_{GA})}$	$k_{GA} K_H$ (mol/g_{cat} bar s)	2.20 E − 06	3.14 E − 06	4.42 E − 06	6.11 E − 06
	K_{GA} (m^3/mol)	6.32 E − 01	5.79 E − 01	5.33 E − 01	4.93 E − 01

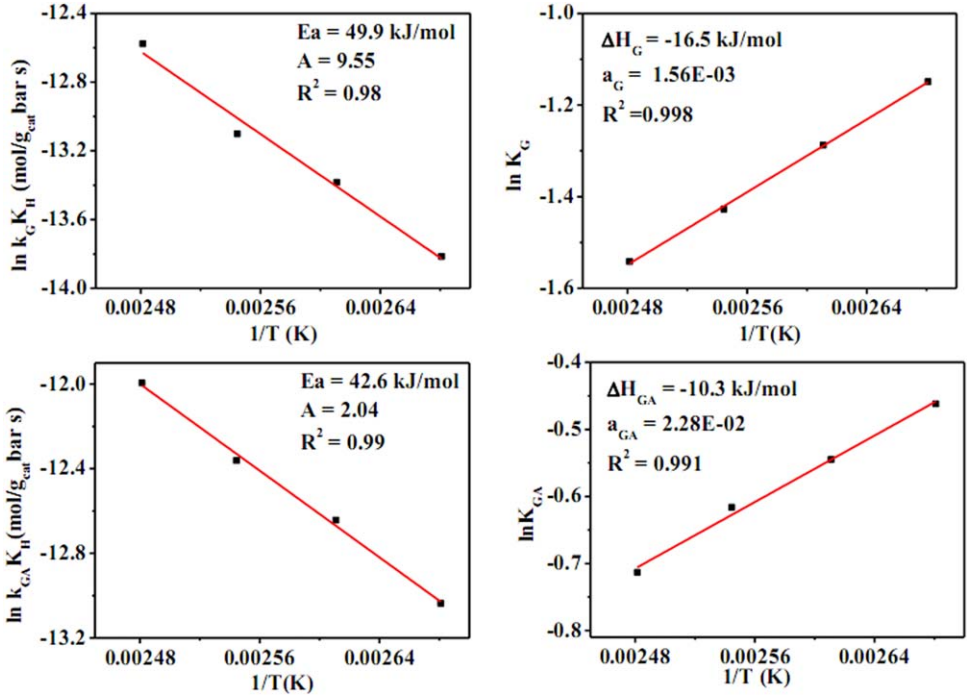

Figure 7. Arrhenius and Van't Hoff parameters for glucose and glycolaldehyde hydrogenation over 1% Ru/C.

[Color figure can be viewed in the online issue, which is available at wileyonlinelibrary.com.]

$$\frac{r_{GA-m}}{r_{GA}} = \frac{1+K_{GA}C_{GA}}{1+K_{GA}C_{GA}+K_{G}C_{G}} < 1 \qquad (75)$$

Furthermore, when the concentrations of glucose and glycolaldehyde in the mixture are comparable, it can be anticipated that the inhibitive effect of competitive hydrogenation between glucose and glycolaldehyde on the glucose hydrogenation is more pronounced because of the smaller adsorption equilibrium constant of glucose (K_G) (Table 1). As predicted by the kinetic model, the experimental results showed that the glucose hydrogenation started to occur only when the glycolaldehyde hydrogenation was almost finished (Figure 8), demonstrating that the presence of glycolaldehyde significantly inhibited the hydrogenation of glucose. The good agreement between the experimental and predicted data validates our kinetic models.

The effect of AMT on the hydrogenation of glucose and glycolaldehyde

The hydrogenation kinetics of individual glucose and glycolaldehyde as well as their mixtures over the Ru/C catalyst has now been successfully modeled with the noncompetitive LHHW model assuming that the surface reaction between the dissociatively adsorbed hydrogen and aldose molecule is the rate-determining step. However, the one-pot conversion of glucose (or cellulose) to EG always takes place under the coexistence of both tungsten compound (e.g., AMT) and Ru/C (or Raney Ni).[35] In this case, investigating whether the presence of AMT affects the hydrogenation kinetics of glucose and glycolaldehyde is important to the final prediction of the EG formation from glucose or cellulose. First, we investigated the effect of AMT on the hydrogenation of

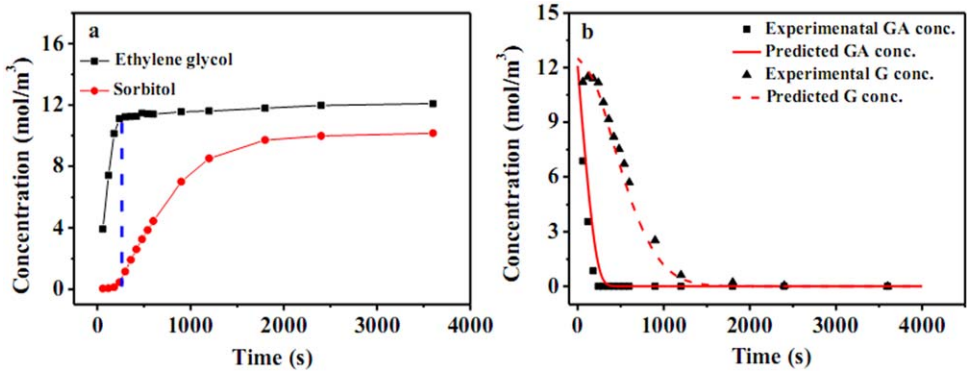

Figure 8. (a) Experimental EG and sorbitol concentration profiles; (b) experimental (dots) and predicted (lines) concentration profiles of glucose and glycolaldehyde.

Reaction conditions: C_{G0} = 10.5 mol/m³, C_{GA0} = 11.0 mol/m³, T = 403 K, P_H = 6 MPa, 0.2 g 1% Ru/C. [Color figure can be viewed in the online issue, which is available at wileyonlinelibrary.com.]

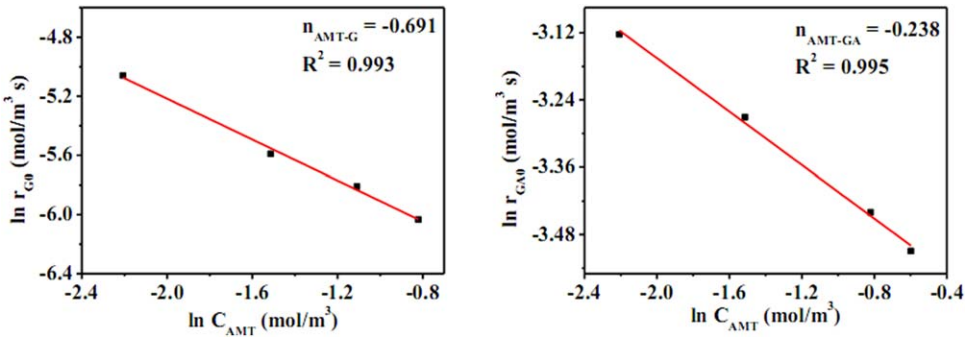

Figure 9. The reaction order of glucose hydrogenation and glycolaldehyde hydrogenation with respect to AMT concentration.

Reaction conditions: $T = 403$ K, $C_{G0} = 4.96$ mol/m^3, $C_{GA0} = 10.4$ mol/m^3, 0.2 g 1% Ru/C, $C_{AMT} = 0.11$–0.55 mol/m^3. [Color figure can be viewed in the online issue, which is available at wileyonlinelibrary.com.]

glucose in the temperature range of 373–403 K. As shown in Figure 5, compared to the case without AMT, the presence of AMT was found to impose a remarkable inhibiting effect on the glucose hydrogenation reaction rate. Moreover, this inhibiting effect appears not to be alleviated at elevated temperatures until 403 K. Similar to glucose, glycolaldehyde hydrogenation was also found to be hindered by the presence of AMT, as shown in Figure 6. Nevertheless, this inhibiting effect was to a much less extent compared with the case of glucose hydrogenation. To provide a more quantitative description of the inhibiting effect of AMT, we used initial reaction rate method to calculate the reaction order with respect to AMT according to the formula

$$\ln\ r_{i0} = n_{AMTi} \ln\ C_{AMT} + \text{Constant} \tag{76}$$

By plotting ln r_{i0}–ln C_{AMT}, one can obtain a straight line whose slope is the reaction order with respect to AMT (n_{AMTi}). The experimental data were obtained at $T = 403$ K, $C_{G0} = 4.96$ mol/m^3, $C_{GA0} = 10.4$ mol/m^3, and $C_{AMT} = 0.11$–0.55 mol/m^3. As shown in Figure 9, the reaction order of AMT was -0.691 and -0.238 for glucose hydrogenation and glycolaldehyde hydrogenation, respectively. Obviously, the inhibiting effect of AMT was much more pronounced on glucose hydrogenation. In other words, for the hydrogenation of glycolaldehyde and glucose mixture, the presence of AMT will result in a more preferential hydrogenation of glycolaldehyde, thus, enhancing the selectivity to EG.

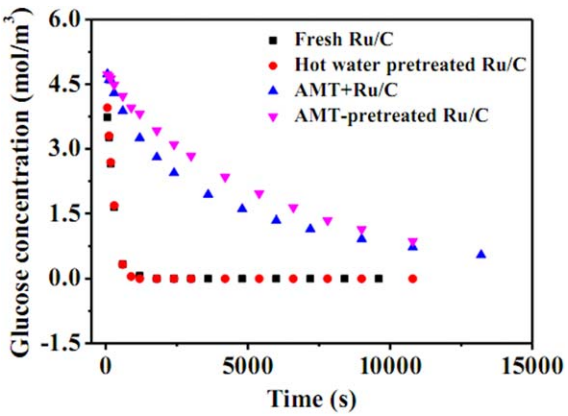

Figure 10. The performance of differently pretreated Ru/C catalyst in the glucose hydrogenation.

Reaction conditions: $C_{G0} = 4.96$ mol/m^3, $T = 403$ K, $P_H = 6$ MPa, 0.2 g 1% Ru/C. For AMT + Ru/C, $C_{AMT} = 0.11$ mol/m^3; for other cases, no AMT was added in the reactor. [Color figure can be viewed in the online issue, which is available at wileyonlinelibrary.com.]

It is interesting to note that the inhibitive effect on aldose hydrogenation was not only found with AMT but also with other tungstic compounds such as tungstic acid, tungsten trioxide, and heteropoly acids. Moreover, the inhibitive effect differed with the type of the tungstic compounds. This inhibiting effect may correlate with the final EG selectivity in the one-pot conversion of glucose or cellulose to EG.

As discussed above, the hydrogenation of glucose and glycolaldehyde was significantly suppressed by the presence of AMT, and this inhibiting effect was more pronounced in the case of glucose. Associated with this prohibiting effect, the kinetic model based on Eqs. 3 and 4 failed to model the experimental data in the presence of AMT, especially in the case of glucose hydrogenation. Therefore, new kinetic model must be developed. To do this, we first investigated the interaction between AMT and Ru/C to see if the Ru surface was poisoned by the adsorption of AMT. The 1% Ru/C catalyst was first submitted to hydrothermal pretreatment with AMT solution at 403 K for 2 h, then it was recovered by filtration and repetitive washing to remove the physically adsorbed AMT. The as-pretreated Ru/C catalyst was put into the reactor for glucose hydrogenation test. As shown in Figure 10, the AMT-pretreated catalyst showed a dramatically reduced activity for glucose hydrogenation in the absence of AMT, as poor as that in the presence of AMT. Conversely, hot water-pretreated Ru/C catalyst did not show any activity decay in the hydrogenation of glucose. These results provided unequivocal evidence that AMT strongly adsorbs on the Ru surface and poisons the catalyst.

In addition to the strong interaction between AMT and Ru/C, glucose and glycolaldehyde chelate also strongly with the AMT. As we have addressed in the previous work,[46] the retro-aldol condensation of glucose occurs with AMT as the catalyst, and the reaction rate is 0.257th-order dependency on the AMT concentration. According to this reaction order, we assume that a stoichiometric ratio of AMT to glucose is 1/4, that is, one glucose molecule can interact with three W atoms (note: 12 W atoms per AMT molecule). It was reported earlier that glucose could form complexes with multinuclear tungstate evidenced by ^{183}W nuclear magnetic resonance (NMR) spectroscopy.[63]

Table 2. Modeling Results of Glucose Hydrogenation Over Ru/C in the Presence of AMT

Model Equation	T (K)	Parameters				R^2
		$k_G K_H$ (mol/g_{cat} bar s)	K_G (m^3/mol)	$K_{G\text{-}AMT}$ (m^3/mol)^5	K_{AMT} (m^3/mol)	
$r_{G-AMT} = k_G \frac{K_H P_H (K_{G-AMT} C_{AMT} C_G^4 + K_G C_G)}{1 + K_{G-AMT} C_{AMT} C_G^4 + K_G C_G + K_{AMT} C_{AMT}}$	373	1.01 E − 06	3.19 E − 01	4.52 E − 02	2.60 E + 02	0.977
	383	1.54 E − 06	2.78 E − 01	2.57 E − 02	2.39 E + 02	0.977
	393	2.28 E − 06	2.43 E − 01	1.50 E − 02	2.21 E + 02	0.974
	403	3.33 E − 06	2.15 E − 01	8.99 E − 03	2.05 E + 02	0.979

Table 3. Modeling Results of Glycolaldehyde Hydrogenation Over Ru/C in the Presence of AMT

Model Equation	T (K)	Parameters				R^2
		$k_{GA} K_H$ (mol/g_{cat} bar s)	K_{GA} (m^3/mol)	K_{GA-AMT} (m^3/mol)^2	K_{AMT} (m^3/mol)	
$r_{GA-AMT} = k_{GA} \frac{K_H P_H (K_{GA-AMT} C_{AMT} C_{GA} + K_{GA} C_{GA})}{1 + K_{GA-AMT} C_{AMT} C_{GA} + K_{GA} C_{GA} + K_{AMT} C_{AMT}}$	373	2.20 E − 06	6.32 E − 01	1.92 E + 01	2.60 E + 02	0.972
	383	3.14 E − 06	5.79 E − 01	1.42 E + 01	2.39 E + 02	0.975
	393	4.42 E − 06	5.33 E − 01	1.07 E + 01	2.21 E + 02	0.979
	403	6.11 E − 06	4.93 E − 01	8.14	2.05 E + 02	0.971

Kinetics of aldoses hydrogenation over dual catalyst (Ru/C + AMT)

By taking into account the inhibitive effect of AMT on the hydrogenation of aldoses, we developed new kinetic models for glucose and glycolaldehyde hydrogenation in the copresence of Ru/C and AMT, as described in Eqs. 50 and 71. With these new models, the *C-t* curves for glucose and glycolaldehyde hydrogenation in the presence of AMT at four different temperatures (358–403 K) are well fitted (Figures 5 and 6), and the equilibrium and kinetic constants ($k_i K_H$, K_i, K_{i-AMT}, K_{AMT}, i = G, GA) are summarized in Tables 2 and 3. It can be seen from Table 2 that the adsorption equilibrium constant of AMT on Ru/C surface (K_{AMT}) is three or four orders of magnitude bigger than that of glucose (K_G) or AMT-complexed glucose ($K_{G\text{-}AMT}$), which is in agreement with the experimental fact that AMT is strongly adsorbed on Ru surface and poisons the catalyst. This poisoning effect leads to the dramatic reduction of glucose hydrogenation reaction rate. Conversely, comparing $K_{G\text{-}AMT}$ and K_G, one can see that the former is one order of magnitude smaller than the latter. Therefore, although the $K_{G\text{-}AMT}$ term appears in the numerator of Eq. 50, its contribution to the reaction rate is negligible. As a consequence, the decrease of the glucose hydrogenation reaction rate is mainly caused by the strong adsorption of AMT on Ru surface.

Similar to the case of glucose hydrogenation in the presence of AMT, 1–4 orders of magnitude higher value of

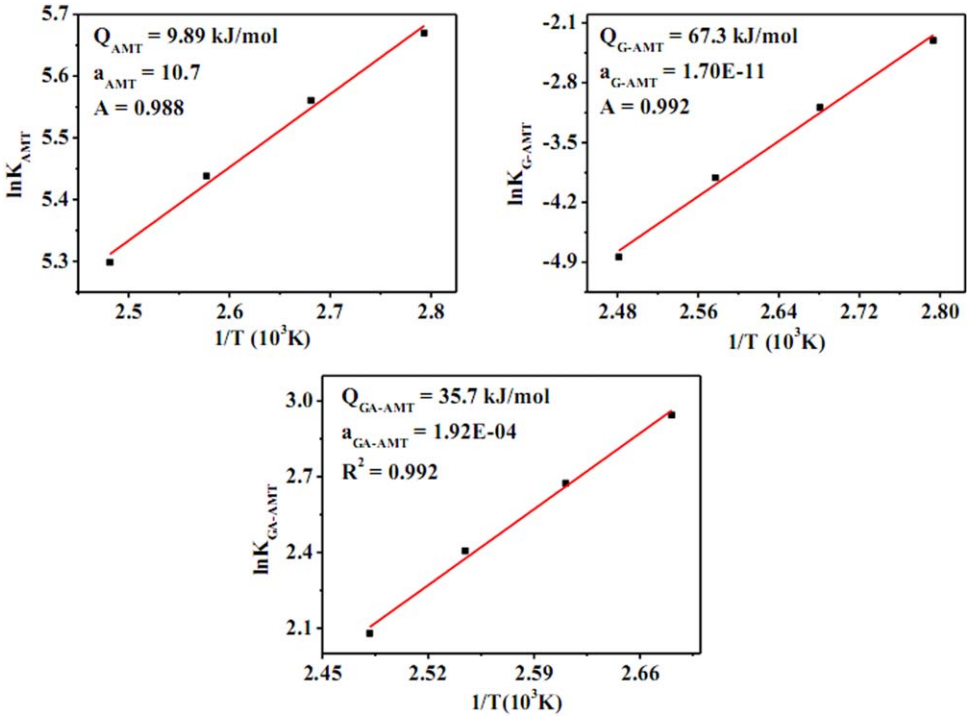

Figure 11. The temperature dependence of K_{AMT}, $K_{G\text{-}AMT}$ and $K_{GA\text{-}AMT}$.

[Color figure can be viewed in the online issue, which is available at wileyonlinelibrary.com.]

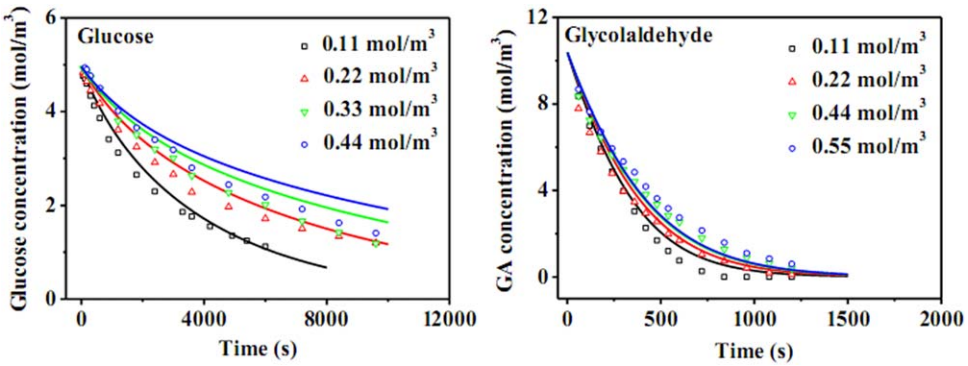

Figure 12. Experimental (dots) and predicted (lines) concentration profiles of glucose and glycolaldehyde at different AMT concentrations.

Reaction conditions: $C_{G0} = 4.96$ mol/m^3, $C_{GA0} = 10.4$ mol/m^3, $T = 403$ K, $P_H = 6$ MPa, 0.2 g 1% Ru/C. [Color figure can be viewed in the online issue, which is available at wileyonlinelibrary.com.]

K_{AMT} than the other equilibrium constants in the denominator indicates a strong inhibiting effect of AMT on the hydrogenation of glycolaldehyde (Table 3). Nevertheless, comparing K_{GA-AMT} and $K_{G\text{-}AMT}$, one can see that the former is 2–3 orders magnitude larger than the latter, and K_{GA-AMT} is even 1–2 orders magnitude larger than K_{GA}. As the term K_{GA-AMT} appears in the numerator of Eq. 71, its contribution to the enhancement of the reaction rate is much larger than the term K_{GA}, thus, alleviating the poisoning effect of AMT on the glycolaldehyde hydrogenation.

On the other hand, the adsorption equilibrium constants K_G, $K_{G\text{-}AMT}$, and K_{AMT} decrease with an increase of the temperature due to the exothermic feature of the adsorption process (Figure 11). However, comparing the other two parameters, one can find that K_{AMT} is only slightly affected by temperature. Considering that K_{AMT} is 3–4 orders of magnitude larger than the other two parameters and thereby affects more significantly the hydrogenation reaction rate of glucose, one can anticipate that the poisoning effect of AMT will be only slightly attenuated at elevated temperatures, which is in good agreement with the experimental results in Figures 5 and 6.

Moreover, these equilibrium constants do not change with AMT concentrations. As shown in Figure 12, the *C-t* curves for glucose and glycolaldehyde hydrogenation at different AMT concentrations can be well modeled with the same set of parameters although slight deviation is observed at high AMT concentrations.

Conclusion

The one-pot conversion of glucose to EG consists of two consecutive reactions, retro-aldol condensation of glucose to glycolaldehyde and the subsequent hydrogenation of glycolaldehyde to EG, which necessitates the employment of a dual catalyst composed of a tungstic compound and a hydrogenation metal. Our previous work revealed that tungstic compounds such as AMT effectively and uniquely catalyze the retro-aldol condensation of glucose to selectively produce glycolaldehyde, while Raney Ni and Ru/C are active and durable catalyst for the subsequent hydrogenation of glycolaldehyde to EG. Meanwhile, both Raney Ni and Ru/C catalysts are also able to catalyze the reaction of glucose hydrogenation to sorbitol that will compete with the reaction of glycolaldehyde hydrogenation resulting in the decrease of EG selectivity.

In this work, the kinetics of glucose and glycolaldehyde hydrogenation over Ru/C with or without the presence of AMT was for the first time studied using a batch reactor in the temperature range of 373–403 K and hydrogen pressure of 6 MPa. To eliminate internal and external diffusion limitations, the kinetic experiments were conducted at an agitation speed of 1100 rpm, 1% Ru/C catalyst loading of 0.2 g, and the particle size of 250–300 mesh. In the absence of AMT, the kinetic data were well modeled based on LHHW mechanism assuming that the surface reaction is rate-determining step and hydrogen and glucose are noncompetitively adsorbed on Ru surface. It was further found that the reaction rate of glycolaldehyde hydrogenation was much faster than that of glucose hydrogenation, which led to the preferential hydrogenation of glycolaldehyde when glucose was copresent with glycolaldehyde in the reaction system. However, in the presence of AMT, it was found that AMT significantly reduced the hydrogenation reaction rate of aldoses (glucose or glycolaldehyde), and this suppressing effect was more pronounced for glucose hydrogenation. The pretreatment of Ru/C with AMT revealed that AMT strongly adsorbed on the Ru/C surface and poisoned the catalyst. Accordingly, new kinetic models taking into account the poisoning effect of AMT on Ru/C catalyst as well as the complexing effect between AMT and aldoses were developed. The modified models could satisfactorily describe the hydrogenation kinetics of glucose and glycolaldehyde in the presence of AMT. The results reported here has provided insightful understanding of the dual effects of the tungstic compound in the one-pot conversion of glucose or cellulose to EG, that is, on one hand it catalyzes the selective cleavage of C—C bonds of glucose to produce glycolaldehyde, and on the other hand it inhibits the hydrogenation of aldoses especially that of glucose by poisoning Ru/C surface. This kinetic study will guide researchers to optimize the ratio of tungsten compounds to Ru/C in the catalyst design.

Finally, it should be mentioned that by combining the two kinetic models, that is, retro-aldol condensation of glucose and hydrogenation of glucose/glycolaldehyde with the dual catalyst AMT + Ru/C, it is possible to obtain an overall kinetic model for the one-pot conversion of glucose to EG. Our preliminary results have shown that both EG and sorbitol yields from glucose conversion can be predicted well

with this overall kinetic model, and this work will be reported as a third article in this journal.

Acknowledgment

This work was financially supported by the National Natural Science Foundation of China (NSFC grants: 21176235, 21373206, and 21206159).

Notation

r_{i0} = the initial rate that incorporate the AMT and Ru/C concentration for glucose or glycolaldehyde hydrogenation reaction, mol/m^3 s
r_G = reaction rate of glucose hydrogenation over Ru/C, mol/g_{cat} s
r_{GA} = reaction rate of glycolaldehyde hydrogenation over Ru/C, mol/g_{cat} s
r_{G-m} = reaction rate of glucose hydrogenation over Ru/C in the case of mixture, mol/g_{cat} s
r_{GA-m} = reaction rate of glycolaldehyde hydrogenation over Ru/C in the case of mixture, mol/g_{cat} s
r_{G-AMT} = reaction rate of glucose hydrogenation over Ru/C in the presence of AMT, mol/g_{cat} s
r_{GA-AMT} = reaction rate of glycolaldehyde hydrogenation over Ru/C in the presence of AMT, mol/g_{cat} s
r_{AMTG} = reaction rate of AMTG hydrogenation over Ru/C, mol/g_{cat} s
r_{AMTG2} = reaction rate of AMTG2 hydrogenation over Ru/C, mol/g_{cat} s
r_{AMTG3} = reaction rate of AMTG3 hydrogenation over Ru/C, mol/g_{cat} s
r_{AMTG3} = reaction rate of AMTG4 hydrogenation over Ru/C, mol/g_{cat} s
r_{AMTGA} = reaction rate of AMTGA hydrogenation over Ru/C, mol/g_{cat} s
k_G = rate constant of glucose hydrogenation, mol/g_{cat} s
k_{GA} = rate constant of glycolaldehyde hydrogenation, mol/g_{cat} s
G = glucose
S = sorbitol
GA = glycolaldehyde
EG = ethylene glycol
C_G = concentration of glucose, mol/m^3
C_S = concentration of sorbitol, mol/m^3
C_{GA} = concentration of glycolaldehyde, mol/m^3
C_{EG} = concentration of ethylene glycol, mol/m^3
C_{AMT} = concentration of ammonium metatungstate (AMT), mol/m^3
C_{AMTG4} = concentration of AMTG4, mol/m^3
C_{AMTGA} = concentration of AMTGA, mol/m^3
K_{AMT} = AMT adsorption equilibrium constant on Ru/C, m^3/mol
K_G = glucose adsorption equilibrium constant on Ru/C, m^3/mol
K_H = dissociative hydrogen adsorption equilibrium constant on Ru/C, 1/bar
K_S = sorbitol adsorption equilibrium constant on Ru/C, m^3/mol
K_{GA} = glycolaldehyde adsorption equilibrium constant on Ru/C, m^3/mol
K_{EG} = ethylene glycol adsorption equilibrium constant on Ru/C, m^3/mol
P_H = hydrogen pressure, bar
m_{cat} = mass of Ru/C catalyste, g_{cat}
n_{AMT-G} = reaction order of glucose hydrogenation with respect to AMT concentration
n_{AMT-GA} = reaction order of glycolaldehyde hydrogenation with respect to AMT concentration
AMT = ammonium metatungstate
AMTG = complex formed by binding AMT with one glucose molecule
AMTG2 = complex formed by binding AMT with two glucose molecules
AMTG3 = complex formed by binding AMT with three glucose molecules
AMTG4 = complex formed by binding AMT with four glucose molecules
AMTGA = complex formed by binding AMT with glycolaldehyde
K_1 = equilibrium constant of adsorbed AMT and glucose, m^3/mol
K_2 = equilibrium constant of adsorbed AMTG and glucose, m^3/mol
K_3 = equilibrium constant of adsorbed AMTG2 and glucose, m^3/mol
K_4 = equilibrium constant of adsorbed AMTG3 and glucose, m^3/mol
K_5 = equilibrium constant of AMT and glucose, m^3/mol
K_6 = adsorption equilibrium constant of AMTG4 over Ru/C, m^3/mol
K_{11} = equilibrium constant of AMT and glycolaldehyde, m^3/mol
K_{12} = adsorption equilibrium constant of AMTGA over Ru/C, m^3/mol
K_{13} = equilibrium constant of adsorbed AMT and glycolaldehyde, m^3/mol
k_7 = rate constant of AMTG4 hydrogenation, mol/g_{cat} s
k_8 = rate constant of AMTG3 hydrogenation, mol/g_{cat} s
k_9 = rate constant of AMTG2 hydrogenation, mol/g_{cat} s
k_{10} = rate constant of AMTG hydrogenation, mol/g_{cat} s
k_{14} = rate constant of adsorbed AMTGA hydrogenation, mol/g_{cat} s
E_{ai} = apparent activation energy for glucose or glycolaldehyde hydrogenation on Ru/C, kJ/mol
A_i = the pre-exponential factor for glucose or glycolaldehyde hydrogenation on Ru/C
ΔH_j = the adsorption enthalpy for glucose or glycolaldehyde, kJ/mol
a_j = the pre-exponential factor in Van 't Hoff equation for glucose or glycolaldehyde
R = universal gas constant (8.3143×10^{-3} kJ/mol/K)
T = temperature, K

Greek letters

ρ_{cat} = catalyst mass per cubic metre (g_{cat}/m^3)
θ_{V1} = catalyst vacant site
θ_{V2} = catalyst vacant site for hydrogen
θ_G = adsorbed glucose species
θ_S = adsorbed sorbitol species
θ_H = adsorbed hydrogen molecule
θ_{GA} = adsorbed glycolaldehyde species
θ_{EG} = adsorbed ethylene glycol species
θ_{AMT} = adsorbed AMT species
θ_{AMTG} = adsorbed AMTG species
θ_{AMTG2} = adsorbed AMTG2 species
θ_{AMTG3} = adsorbed AMTG3 species
θ_{AMTG4} = adsorbed AMTG4 species
θ_{AMTGA} = adsorbed AMTGA species

Literature Cited

1. Huber GW, Iborra S, Corma A. Synthesis of transportation fuels from biomass: chemistry, catalysts, and engineering. *Chem Rev*. 2006;106:4044–4098.
2. Corma A, Iborra S, Velty A. Chemical routes for the transformation of biomass into chemicals. *Chem Rev*. 2007;107:2411–2502.
3. Stöcker M. Biofuels and biomass-to-liquid fuels in the biorefinery: catalytic conversion of lignocellulosic biomass using porous materials. *Angew Chem Int Ed*. 2008;47:9200–9211.
4. Dhepe P, Fukuoka A. Cellulose conversion under heterogeneous catalysis. *ChemSusChem*. 2008;1:96–97.
5. Rinaldi R, Schüth F. Design of solid catalysts for the conversion of biomass. *Energy Environ Sci*. 2009;2:610–626.
6. Alonso DM, Bond JQ, Dumesic JA. Catalytic conversion of biomass to biofuels. *Green Chem*. 2010;12:1493–1513.
7. Marquardt W, Harwardt A, Hechinger M, Kraemer K, Viell J, Voll A. The biorenewables opportunity—toward next generation process and product systems. *AIChE J*. 2010;56(9):2228–2235.
8. Mussatto SI, Dragone G, Guimarães P, Silva J, Carneiro L, Roberto I, Vicente A, Domingues L, Teixeira J. Technological trends, global market, and challenges of bio-ethanol production. *Biotechnol Adv*. 2010;28:817–830.
9. Zhou C, Xia X, Lin C, Tong D, Beltramini J. Catalytic conversion of lignocellulosic biomass to fine chemicals and fuels. *Chem Soc Rev*. 2011;40:5588–5617.
10. Kobayashi H, Komanoya T, Guha SK, Hara K, Fukuoka A. Conversion of cellulose into renewable chemicals by supported metal catalysis. *Appl Catal A*. 2011;409:13–20.
11. Gallezot P. Conversion of biomass to selected chemical products. *Chem Soc Rev*. 2012;41:1538–1558.
12. Peng B, Yuan X, Zhao C, Lercher JA. Stabilizing catalytic pathways via redundancy: selective reduction of microalgae oil to alkanes. *J Am Chem Soc*. 2012;134:9400–9405.
13. Wang Y, Deng W, Wang B, Zhang Q, Wan X, Tang Z, Wang Y, Zhu C, Cao Z, Wang G, Wan H. Chemical synthesis of lactic acid from cellulose catalysed by lead(II) ions in water. *Nat Commun*. 2013;4:1–7.
14. Huang Y, Fu Y. Hydrolysis of cellulose to glucose by solid acid catalysts. *Green Chem*. 2013;15:1095–1111.

15. Modenbach AA, Nokes SE. Enzymatic hydrolysis of biomass at high-solids loadings—a review. *Biomass Bioenergy*. 2013;56:526–544.
16. Daoutidis P, Marvin WA, Rangarajan S, Torres AI. Engineering biomass conversion processes: a systems perspective. *AIChE J*. 2013; 59:3–18.
17. Wang Y, Jin F, Sasaki M, Wahyudiono, Wang F, Jing Z, Goto M. Selective conversion of glucose into lactic acid and acetic acid with copper oxide under hydrothermal conditions. *AIChE J*. 2013;59: 2096–2104.
18. Wang J, Ren J, Liu X, Lu G, Wang Y. High yield production and purification of 5-Hydroxymethylfurfural. *AIChE J*. 2013;59:2558–2566.
19. Joffres B, Lorentz C, Vidalie M, Laurenti D, Quoineaud AA, Charon N, Daudin A, Quignard A, Geantet C. Catalytic hydroconversion of a wheat straw soda lignin: characterization of the products and the lignin residue. *Appl Catal B*. 2014;145:167–176.
20. Yoshikawa T, Shinohara S, Yagi T, Ryumon N, Nakasaka Y, Tago T, Masuda T. Production of phenols from lignin-derived slurry liquid using ironoxide catalyst. *Appl Catal B*. 2014;146:289–297.
21. Li G, Li N, Yang J, Li L, Wang A, Wang X, Cong Y, Zhang T. Synthesis of renewable diesel range alkanes by hydrodeoxygenation of furans over Ni/Hβ under mild conditions. *Green Chem*. 2014;16: 594–599.
22. Huang Z, Chen J, Jia Y, Liu H, Xia C, Liu H. Selective hydrogenolysis of xylitol to ethylene glycol and propylene glycol over copper catalysts. *Appl Catal B*. 2014;147:377–386.
23. Juodeikiene G, Cernauskas D, Vidmantiene D, Basinskiene L, Bartkiene E, Bakutis B, Baliukoniene V. Combined fermentation for increasing efficiency of bioethanol production from Fusarium sp. contaminated barley biomass. *Catal Today*. 2014;223:108–114.
24. Li M, Li G, Li N, Wang A, Dong W, Wang X, Cong Y. Aqueous phase hydrogenation of levulinic acid to 1,4-pentanediol. *Chem Commun*. 2014;50:1414–1416.
25. Xi J, Zhang Y, Ding D, Xia Q, Wang J, Liu X, Lu G, Wang Y. Catalytic production of isosorbide from cellulose over mesoporous niobium phosphate-based heterogeneous catalysts via a sequential process. *Appl Catal A*. 2014;469:108–115.
26. Komanoya T, Kobayashi H, Hara K, Chun W, Fukuoka A. Kinetic study of catalytic conversion of cellulose to sugar alcohols under low-pressure hydrogen. *ChemCatChem*. 2014;6:230–236.
27. Chung P, Charmot A, Olatunji-Ojo OA, Durkin KA, Katz A. Hydrolysis catalysis of miscanthus xylan to xylose using weak-acid surface sites. *ACS Catal*. 2014;4:302–310.
28. Wen C, Barrow E, Hattrick-Simpers J, Lauterbach J. One-step production of long-chain hydrocarbons from waste-biomass-derived chemicals using bi-functional heterogeneous catalysts. *Phys Chem Chem Phys*. 2014;16:3047–3054.
29. Saidi M, Samimi F, Karimipourfard D, Nimmanwudipong T, Gates BC, Rahimpour MR. Upgrading of lignin-derived bio-oils by catalytic hydrodeoxygenation. *Energy Environ Sci*. 2014;7:103–129.
30. Saha B, Abu-Omar MM. Advances in 5-hydroxymethylfurfural production from biomass in biphasic solvents. *Green Chem*. 2014;16: 24–38.
31. Liu D, Chen EYX. Diesel and alkane fuels from biomass by organocatalysis and metal–acid tandem catalysis. *ChemSusChem*. 2013;6: 2236–2239.
32. Ji N, Zhang T, Zheng M, Wang A, Wang H, Wang X, Chen J. Direct catalytic conversion of cellulose into ethylene glycol using nickel-promoted tungsten carbide catalysts. *Angew Chem Int Ed*. 2008;47:8510–8513.
33. Liu Y, Luo C, Liu H. Tungsten trioxide promoted selective conversion of cellulose into propylene glycol and ethylene glycol on a ruthenium catalyst. *Angew Chem Int Ed*. 2012;51:3249–3253.
34. Wang X, Meng L, Wu F, Jiang Y, Wang L, Mu X. Efficient conversion of microcrystalline cellulose to 1, 2-alkanediols over supported Ni catalysts. *Green Chem*. 2012;14:758–765.
35. Wang A, Zhang T. One-pot conversion of cellulose to ethylene glycol with multifunctional tungsten-based catalysts. *Acc Chem Res*. 2013;46:1377–1386.
36. Xiao Z, Jin S, Pang M, Liang C. Conversion of highly concentrated cellulose to1,2-propanediol and ethylene glycol over highly efficient CuCr catalysts. *Green Chem*. 2013;15:891–895.
37. Li J, Liu L, Liu Y, Li M, Zhu Y, Liu H, Kou Y, Zhang J, Han Y, Ma D. Direct conversion of cellulose using carbon monoxide and water on a Pt–Mo2C/C catalyst. *Energy Environ Sci*. 2014;7:393–398.
38. Zhang Y, Wang A, Zhang T. A new 3D mesoporous carbon replicated from commercial silica as a catalyst support for direct conversion of cellulose into ethylene glycol. *Chem Commun*. 2010;46:862–864.
39. Zheng M, Wang A, Ji N, Pang J, Wang X, Zhan T. Transition metal–tungsten bimetallic catalysts for the conversion of cellulose into ethylene glycol. *ChemSusChem*. 2010;3:63–66.
40. Pang J, Zheng M, Wang A, Zhang T. Catalytic hydrogenation of corn stalk to ethylene glycol and 1, 2-propylene glycol. *Ind Eng Chem Res*. 2011;50:6601–6608.
41. Zhou L, Wang A, Li C, Zheng M, Zhang T. Selective production of 1,2-propyleneglycol from jerusalem artichoke tuber using Ni-W2C/AC catalysts. *ChemSusChem*. 2012;5:932–938.
42. Tai Z, Zhang J, Wang A, Zheng M, Zhang T. Temperature-controlled phase-transfer catalysis for ethylene glycol production from cellulose. *Chem Commun*. 2012;48:7052–7054.
43. Li C, Zheng M, Wang A, Zhang T. One-pot catalytic hydrocracking of raw woody biomass into chemicals over supported carbide catalysts: simultaneous conversion of cellulose, hemicellulose and lignin. *Energy Environ Sci*. 2012;5:6383–6390.
44. Ji N, Zheng M, Wang A, Zhang T, Chen J. Nickel-promoted tungsten carbide catalysts for cellulose conversion: effect of preparation methods. *ChemSusChem*. 2012;5:939–944.
45. Tai Z, Zhang J, Wang A, Pang J, Zheng M, Zhang T. Catalytic conversion of cellulose to ethylene glycol over a low-cost binary catalyst of Raney Ni and tungstic acid. *ChemSusChem*. 2013;6: 652–658.
46. Zhang J, Hou B, Wang A, Li Z, Wang H, Zhang T. Kinetic study of retro-aldol condensation of glucose to glycolaldehyde with ammonium metatungstate as the catalyst. *AIChE J*. 2014;60:3804–3813.
47. Ahmed MJ. Kinetics studies of D-glucose hydrogenation over activated charcoal supported platinum catalyst. *Heat Mass Transfer*. 2012;48:343–347.
48. Brahme PH, Doraiswamy LK. Modelling of a slurry reaction. Hydrogenation of glucose on Raney nickel. *Ind Eng Chem Process Des Dev*. 1976;15:130–137.
49. Wisniak J, Simon R. Hydrogenation of glucose, fructose, and their mixtures. *Ind Eng Chem Prod Res Dev*. 1979;18:50–57.
50. Turek F, Chakrabarti RK, Lange R, Geike R, Flock W. On the experimental study and scale-up of three-phase catalytic reactors: hydrogenation of glucose on nickel catalyst. *Chem Eng Sci*. 1983;38: 275–283.
51. Déchamp N, Gamez A, Perrard A, Gallezot P. Kinetics of glucose hydrogenation in a trickle-bed reactor. *Catal Today*. 1995;24:29–34.
52. Crezee E, Hoffer BW, Berger RJ, Makkee M, Kapteijn F, Moulijn JA. Three-phase hydrogenation of D-glucose over a carbon supported ruthenium catalyst—mass transfer and kinetics. *Appl Catal A*. 2003;251:1–17.
53. Herrera V, Oladele O, Kordás K, Eränen K, Mikkola J, Murzin DY, Salmi T. Sugar hydrogenation over a Ru/C catalyst. *J Chem Technol Biotechnol*. 2011;86:658–668.
54. Kuusisto J, Mikkola J, Sparv M, Wärnå J, Heikkilä H, Perälä R, Väyrynen J, Salmi T. Hydrogenation of lactose over sponge nickel catalysts–kinetics and modeling. *Ind Eng Chem Res*. 2006;45:5900–5910.
55. Kuusisto J. Mikkola JP. Sparv M. Wärnå J, Karhu H, Salmi T. Kinetics of the catalytic hydrogenation of D-lactose on a carbon supported ruthenium catalyst. *Chem Eng J*. 2008;139:69–77.
56. Chang NS, Aldrett S, Holtzapple MT, Davison RR. Kinetic studies of ketone hydrogenation over Raney nickel catalyst. *Chem Eng Sci*. 2000;55:5721–5732.
57. Kishida H, Jin F, Yan X, Moriya T, Enomoto H. Formation of lactic acid from glycolaldehyde by alkaline hydrothermal reaction. *Carbohydr Res*. 2006;341:2619–2623.
58. Delidovich IV, Simonov AN, Pestunova OP, Parmon VN. Catalytic condensation of glycolaldehyde and glyceraldehyde with formaldehyde in neutral and weakly alkaline aqueous media: kinetics and mechanism. *Kinet Catal*. 2009;50:297–303.
59. Kim HJ, Ricardo A, Illangkoon HI, Kim MJ, Carrigan MA, Frye F, Benner SA. Synthesis of carbohydrates in mineral-guided orebiotic cycles. *J Am Chem Soc*. 2011;133:9457–9468.
60. Dusselier M, Wouwe PV, Smet SD, Clercq RD, Verbelen L, Puyvelde PV, Prez FE, Sels BF. Toward functional polyester building blocks from renewable glycolaldehyde with Sn cascade catalysis. *ACS Catal*. 2013;3:1786–1800.

61. Busetto L, Fabbri D, Fabbri D, Salmi M, Torri C, Zanotti V. Application of the Shvo catalyst in homogeneous hydrogenation of bio-oil obtained from pyrolysis of white poplar: new mild upgrading conditions. *Fuel*. 2011;90:1197–1207.
62. Kemmer G, Keller S. Nonlinear least-squares data fitting in Excel spreadsheets. *Nat Protoc*. 2010;5:267–280.
63. Chapelle S, Verchère J. Tungstate complexes of aldoses and ketoses of the lyxo series. Multinuclear NMR evidence for chelation by one or two oxygen atoms borne by the side chain of the furanose ring. *Carbohydr Res*. 1995;277:39–50.

Manuscript received Mar. 6, 2014, and revision received Sep. 3, 2014.